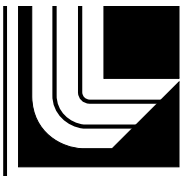

LAWRENCE
LIVERMORE
NATIONAL
LABORATORY

UCRL-JRNL-207045

Quantifying the Sensitivity of Superconducting High-Resolution X-Ray Spectrometers

O.B. Drury, S. Friedrich

October 5, 2004

Physica Status Solidi (c)

Quantifying the Sensitivity of Superconducting High-Resolution X-Ray Spectrometers

Owen B. Drury, and Stephan Friedrich

***Abstract*—Superconducting tunnel junction (STJ) X-ray spectrometers have been developed for synchrotron-based high-resolution soft X-ray spectroscopy. We are quantifying the improvements in sensitivity that STJ spectrometers can offer for the analysis of dilute specimens over conventional semiconductor and grating spectrometers. We present analytical equations to quantify the improvements in terms of spectrometer resolution, detection efficiency and count rate capabilities as a function of line separation and spectral background. We discuss the implications of this analysis for L-edge spectroscopy of first-row transition metals.**

***Index Terms*—Sensitivity, superconducting devices, superconducting tunnel junctions, X-ray spectroscopy detectors**

I. Introduction

SUPERCONDUCTING tunnel junction (STJ) X-ray spectrometers operating at temperatures around ~0.1 K provide an order of magnitude higher energy resolution than conventional Ge or Si(Li) semiconductor detectors and an order of magnitude higher detection efficiency than grating spectrometers [1]-[4]. Over the last decade, STJ spectrometers have been developed for chemical analysis of dilute samples by high-resolution X-ray absorption spectroscopy (XAS) [5]. Fluorescence-detected XAS is the preferred technique to analyze dilute elements, since the sensitivity can be greatly increased if the associated weak characteristic emission lines can be separated from the X-ray background due to other elements in the sample [6]. STJ spectrometers are preferred when line-overlap precludes the use of Ge or Si(Li) detectors, and when grating spectrometers do not have the detection efficiency to collect enough signal counts within an acceptable time. Short data acquisition times are essential for analyzing biological samples that are affected by radiation damage. STJ spectrometers are thus particularly useful for the analysis of dilute first-row transition metals by L-edge spec-troscopy [7], or for K-edge spectroscopy of light elements [8].

In this paper we quantify the improvements in sensitivity that STJ spectrometers can provide over conventional semiconductor or grating spectrometers for soft X-ray spectroscopy. This analysis helps

1) to determine which spectrometer provides the highest sensitivity for a given application,
2) to assess how close a measurement is to the theoretically best achievable signal-to-noise ratio, and
3) to guide future STJ detector development.

II. Spectrometer Sensitivity

A. Statistical Limits

Consider the case when the detection of a fluorescence signal from an element x of interest at energy E_x with total counts N_x is affected by a nearby fluorescence line at energy E_y from element y with total counts N_y. We assume that the spectrometer response is Gaussian, and that it is adequately characterized by its full-width at half maximum ΔE_{FWHM}. Also consider that the signal detection is affected by a constant spectral background B, either due to elastic scatter of the incident beam or due to non-idealities of the spectrometer response function. In this case, the limiting statistical contribution to the measurement errors σ_x and σ_y can be determined analytically [9] according to

$$\sigma_x^2 = aB + bN_x + cN_y$$
$$\sigma_y^2 = aB + bN_y + cN_y \qquad (1)$$
$$\text{with } a = \frac{\Delta E_{FWHM}\sqrt{\pi}}{\sqrt{2\ln 2}(1-d^2)},\ b = \frac{2-4d^{7/3}+2d^{10/3}}{\sqrt{3}(1-d^2)^2},$$
$$c = \frac{2d^{4/3}-4d^{7/3}+2d^2}{\sqrt{3}(1-d^2)^2},\ d = e^{-2\ln 2(E_x-E_y)^2/\Delta E_{FWHM}^2}.$$

Equation (1) describes the statistical precision in the limiting case that systematic errors are negligible. It quantifies this limit in terms of line separation E_x - E_y and detector resolution ΔE_{FWHM}, which enter through the parameter d. The parameter a describes the influence of the background B on the precision, and correctly leads to $\sigma_{x,y} \propto \sqrt{\Delta E_{FWHM}}$ when background statistics dominate the spectrum, i.e. in the limit $d \rightarrow 0$ and $B >> (N_x + N_y)$. The parameter c quantifies the influence of the overlap of one line on the precision for

Manuscript received October 4, 2004. This work was supported in part by the National Science Foundation under grant DMR-0114216, and by the U.S. Department of Energy, Office of Non-Proliferation Research and Engineering, NA-22, under grant LL035-DP. This work was performed under the auspices of the U.S. Department of Energy by University of California Lawrence Livermore National Laboratory under contract No. W-7405-Eng-48.

O. B. Drury and S. Friedrich are with the Advanced Detector Group at the Lawrence Livermore National Laboratory, L-270, Livermore, CA 94550 (corresponding author: S. Friedrich: 925-423-1527; fax: 925-424-5512; e-mail: friedrich1@llnl.gov).

measuring the other line. As expected, $c \rightarrow 0$ for well separated lines, i. e. $d \rightarrow 0$ for $E_x - E_y >> \Delta E_{FWHM}$.

It is now possible to compare the sensitivity of different X-ray spectrometers in terms of their energy resolution, count rate capabilities and detection efficiencies. We focus on the analysis of dilute samples, the primary motivation to develop STJ spectrometers for synchrotron science. Unless explicitly mentioned, we assume that there are $N = 10^7$ counts total in the spectrum, roughly corresponding to operating a 30-pixel detector array at rate of ~20,000 counts/s per pixel and an acquisition time τ ~15 s, that the signal N_x from the element x of interest constitutes only 1% of that total, and that the background B is negligible. Assuming that the fluorescence yield of all elements in the sample is roughly comparable, a signal level of 1% roughly corresponds to a concentration of 1000 ppm of the element of interest, since the absorption by that element increases significantly at its absorption edges.

B. *Sensitivity vs Energy Resolution*

Figure 1 shows the signal-to-noise (S/N) ratio N_x/σ_x according to equation (1) as a function of energy resolution for different signal levels N_x corresponding to different concentrations of element x in the sample. If the spectrometer resolution is sufficient to fully separate the two lines, the signal-to-noise ratio is independent of energy resolution and approaches $1/\sqrt{N_x}$, since $\sigma_x \rightarrow \sqrt{N_x}$ according to Poisson's statistics. The energy resolution ΔE_{FWHM} starts to matter only when it is comparable the line separation $E_y - E_x$, in which case the S/N ratio degrades roughly proportional to ΔE_{FWHM} or ΔE^2_{FWHM} depending on the relative magnitude of the lines and the degree of line overlap [10]. In general, high-resolution STJ spectrometers are therefore only preferred for soft X-rays where line overlap is more common, while conventional high-efficiency Ge spectrometers are preferred for hard X-rays.

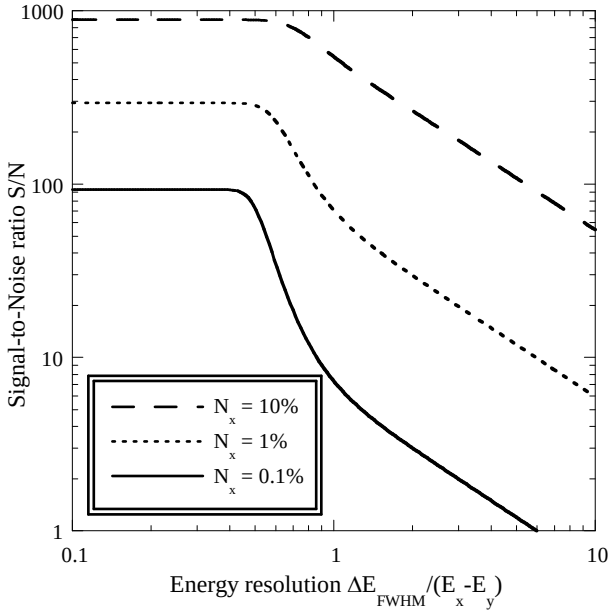

Fig. 1: Signal-to-noise ratio for detecting a weak signal N_x at E_x as a function of energy resolution ΔE_{FWHM} (in units of the line separation $E_y - E_x$ of that signal from a nearby emission line at E_y). The plot shows the limiting S/N ratio when the signal N_x is 10%, 1% and 0.1% of the total ($N = 10^7$). A S/N ratio above 100 is desirable for precise chemical analysis, and S/N ratios below 10 are marginal. A S/N ratio of 3 is often called the detection limit.

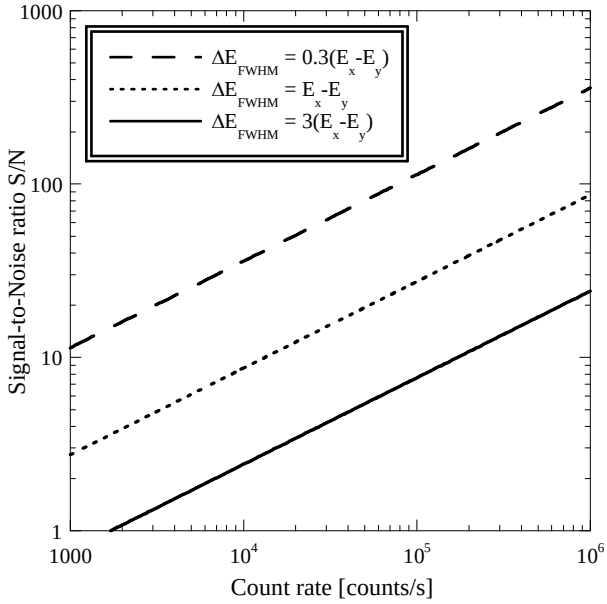

Fig. 2: Signal-to-noise ratio as a function of total count rate for different degrees of line overlap, a signal rate of 1% and an acquisition time of 15 s.

C. *Sensitivity vs Count Rate*

In X-ray spectroscopy, there is usually a trade-off between spectrometer energy resolution and count rate. High data acquisition rates require shorter shaping times to reduce pile-up and thus increase the electronic noise. Also, for weak excitation sources or low X-ray fluorescence yield, spectrometers often do not collect sufficiently many counts to be operated at their maximum rate. Figure 2 shows how the S/N ratio improves with count rate for a constant data acquisition time τ = 15 s and different degrees of line overlap $\Delta E_{FWHM}/(E_y - E_x)$. For a given τ the S/N ratio improves with the square root of the count rate because of Poisson's statistics. The degree of line overlap then determines the absolute value of the S/N ratio that can be attained within the acquisition time τ.

D. *Sensitivity vs Detection Efficiency*

Ge, STJ and grating spectrometers have vastly different total detection efficiencies, ranging form ~10^{-6} for high-resolution gratings to ~10^{-1} for large Ge detector arrays. The term "efficiency" is used here to describe the fraction of the total number of fluorescence X-rays emitted form the sample that are recorded in the spectrum. It is given by the product of the solid angle $\Omega/4\pi$ that the spectrometer subtends and the quantum efficiency η of the detection process. Figure 3 demonstrates how the detection efficiency affects the achievable S/N ratio for different degrees of line overlap. The simulation assumes typical values of the incident flux (I_0 =

10^{12} photons/s), the fluorescence yield ($\varepsilon = 10^{-3}$ for soft X-rays) so that there is a total fluorescence flux of 10^9 photons/s. As expected, the S/N ratio increases with the square root of the detection efficiency because of Poisson's statistics. However, it decreases more rapidly with line overlap (cf. Fig.1). From a practical point of view this implies that the spectrometer should be used that has the highest efficiency and

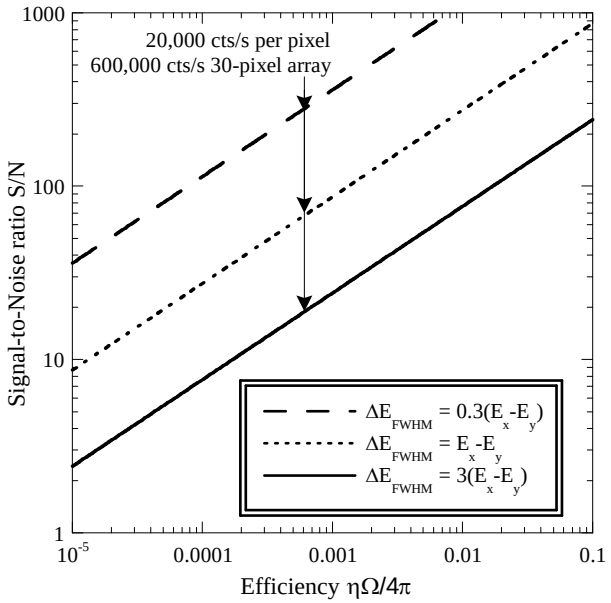

Fig. 3: Signal-to-noise ratio as a function of detection efficiency for different degrees of line overlap and a signal rate of 1% of the total. The arrows indicate a total count rate of 20,000 counts/s per detector pixel.

can still fully separate the lines of interest. Figure 3 is similar to figure 2, in the sense that the improved S/N ratio relies on improved counting statistics. One difference is that the efficiency cannot be increased arbitrarily without exceeding the maximum count rate capabilities of the spectrometer. This is indicated by the arrow in figure 3 where the total count rate exceeds 20,000 counts/s per detector pixel.

E. Sensitivity vs Background

So far we have assumed that the spectral background B is negligible. Many spectrometers have a peak-to-background (P/B) ratio of 200 or better, so this approximation is often justified. However, for dilute samples, small spectral artifacts,

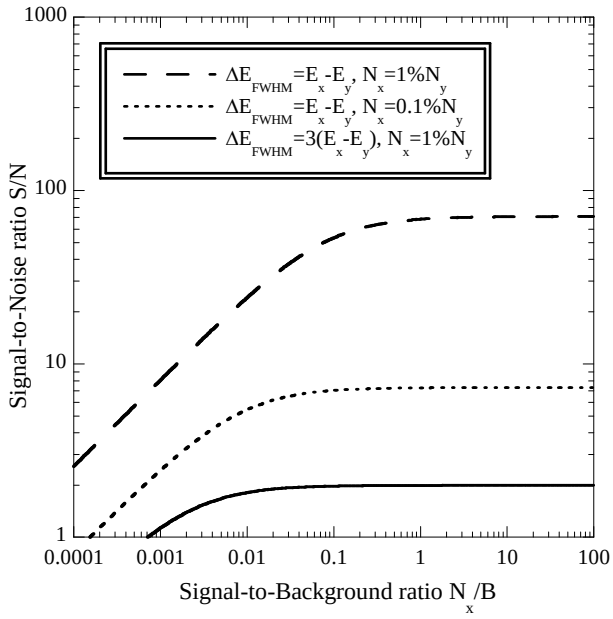

Fig. 4: Signal-to-noise ratio as a function of spectral background for different degrees of line overlap and a signal rate of 1% of the total.

a finite background due to dark counts, or elastic scatter of the incident beam can dramatically decrease the spectrometer sensitivity. This is quantified in figure 4. As before, we assume a total number of counts $N = 10^7$, and a fraction of 1% or 0.1% in the signal, i.e. $N_x = 10^5$ or 10^4. In the background-dominated case, the S/N ratio improves with $\sqrt{\Delta E_{FWHM}}$, since the signal counts are concentrated in a smaller energy range. This energy range decreases with ΔE_{FWHM}, and since the background is assumed constant and dominant, the error decreases with $\sqrt{\Delta E_{FWHM}}$.

F. Sensitivity vs Acquisition Time

Ultimately, it is always possible to compensate for the finite energy resolution of a spectrometer through longer acquisition times, subject only to the constraints of radiation damage and/or patience. The improvements in S/N ratio are shown in figure 5 for data acquisition times between 1 s and 5 min. This range was chosen since typical X-ray absorption spectra involve stepping the excitation energy through an absorption edge of the element of interest, and acquiring a fluorescence spectrum at each energy. Typical absorption spectra involve ~200 steps, so that an acquisition time of 5 min per excitation energy corresponds to a total scan time of 10 hours. Again, we assume an acquisition rate of $6 \cdot 10^5$ counts/s, corresponding to 30 detector elements operating at 20,000 counts/s each.

Figure 5 shows that an acquisition time of 10 to 15 s per step is sufficient to analyze elements at a concentration of ~1000 ppm ($\Rightarrow N_x = 1\%$) in a single ~1 hour XAS scan and obtain an adequate S/N ratio above 100 [5, 7]. More dilute samples with a concentration of ~10 ppm ($\Rightarrow N_x = 0.01\%$) currently require longer acquisition times of at least 10 hours, achieved by averaging the results of several scans. In the future, this time can be greatly reduced using larger detector arrays with higher efficiency and count rate capabilities.

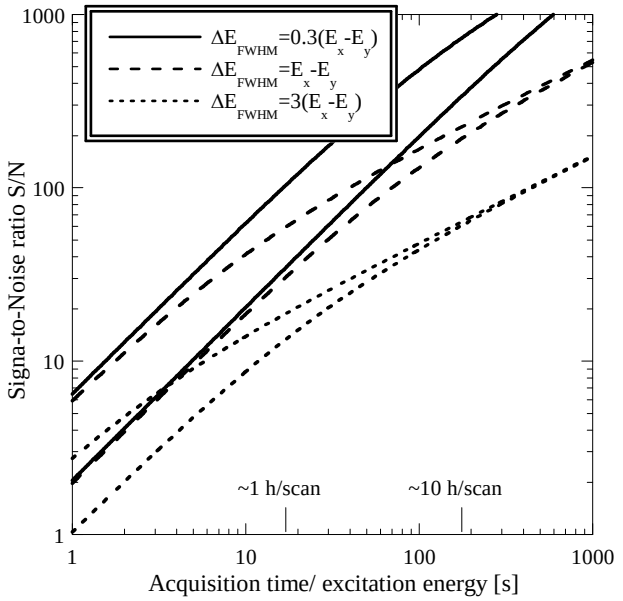

Fig. 5: Signal-to-noise ratio as a function of data acquisition time and a signal strength of 1% (upper) and 0.01% of the total (lower line of each pair) for different degrees of line overlap. These signal rates roughly correspond to a sample concentration of 1000 and 10 ppm, respectively.

III. Spectrometer Comparison

A. Scientific Relevance

We apply this analysis to synchrotron-based fluorescence-detected XAS of dilute samples. As an example, we consider the first-row transition metals Sc, Ti, V, Cr, Mn Fe, Co, Ni, Cu and Zn. They are comparably abundant in the earth's crust, and the elements from Ti to Cu can be present in more than one oxidation state. They play important roles as trace elements in the metabolic processes in cells, or as dopants in novel semiconducting or magnetic materials. Some of them, like Cr, Mn and Fe, are also of significant environmental concern because of their toxicity or their oxidative or absorptive influence on other environmental contaminations. Scientific questions often center on the chemical state of the transition metal and its changes under specific conditions, and L-edge XAS is a sensitive element-specific probe of that state [11, 12]. The L-series X-ray emission lines of first row transition metals range from 395 eV for Sc to 1012 eV for Zn. Unfortunately, there are often line overlap problems in that energy range, e.g. due to strong carbon K and oxygen K fluorescence at 277 and 525 eV. Here we discuss the trade-offs between energy resolution, count rate and efficiency when analyzing these transition metals by XAS, and quantify the sensitivity different spectrometer types can attain.

B. Signal Rates

If a dilute sample is illuminated at the synchrotron with a monochromatic X-ray beam with energy E_0 and $I_0 = 10^{12}$ photons/s, the measured signal N_x at energy E_x from element x within an acquisition time τ is given by [6]

TABLE I
Spectrometer Comparison

Detector	Resolution ΔE_{FWHM}	Count rate *counts/s*	Efficiency $\eta\,\Omega/4\pi$	P/B ratio
Ge (typical)	130 eV	$3{\cdot}10^5$	0.1	50:1
Ge (best)	60 eV	$3{\cdot}10^4$	0.03	200:1
Ge (ideal)	40 eV	10^7	0.1	1,000:1
STJ (typical)	20 eV	10^5	10^{-4}	200:1
STJ (best)	10 eV	10^6	10^{-3}	1,000:1
STJ (ideal)	5 eV	10^7	10^{-2}	5,000:1
Grating (typ.)	0.5 eV	10^5	10^{-6}	200:1
Grating (best)	0.2 eV	10^6	10^{-5}	1,000:1
Gr. with optic	0.2 eV	10^6	$3{\cdot}10^{-4}$	200:1
Grating (ideal)	0.1 eV	10^7	10^{-3}	5,000:1

Performance at an X-ray energy of 0.5 keV. All values are approximate.

$$N_x = I_0 \tau \cdot \frac{\mu_x(E_0) \cdot \varepsilon_x}{\mu_{tot}(E_0) + \mu_{tot}(E_x)} \cdot \frac{\Omega}{4\pi} \cdot \eta \,. \qquad (2)$$

Here μ_x is the absorption coefficient of the element x and μ_{tot} is the total absorption efficient of the sample, ε_x is the fluorescence yield, $\Omega/4\pi$ is the solid angle the detector covers, and η is the detector's quantum efficiency. If all elements in the sample had the same absorption efficiency and fluorescence yield, the term $\mu_x(E_0)/(\mu_{tot}(E_0)+\mu_x(E_x))$ would be roughly equal to the concentration of element x in the sample. In practice it is about an order of magnitude higher since the element x has an increased absorption coefficient at its absorption edges.

C. Spectrometer Characteristics

Both Ge, STJ and grating spectrometers can be used for fluorescence-detected XAS. These spectrometers vary greatly with respect to energy resolution, count rate capabilities and detection efficiency. Table 1 summarizes their performance at 0.5 keV for a) typical, b) state-of-the art, and c) theoretically ideal instruments.

The "typical" Ge detector describes the original average performance of our commercial 30-element Ge spectrometer [13]. The currently "best" Ge detector, chosen solely for its achieved resolution at 0.5 keV, is a single channel Ge detector optimized for low-energy performance [14, 15]. The "ideal" Ge detector would combine Fano-limited resolution with 30-channel array capability. Its peak-to-background (P/B) ratio is limited by a ~15 nm dead layer at the contact electrode [15].

The "typical" STJ detector describes the performance our current 9-pixel STJ spectrometer during past routine operation [5]. The "best" STJ combines achieved energy resolution [16] and P/B ratios [17, 18] with the efficiency and count rate capabilities of our current 36-pixel upgrade (figure 6). The "ideal" STJ combines Fano-limited resolution [19] with a future upgrade to ~1000 pixels. There is no unavoidable dead layer in STJ detectors. While the small detector size limits its solid angle coverage, it allows placing most of the STJ array at an angle of 90° to the incident beam, thereby limiting elastic scatter and maintaining a high P/B ratio.

Grating spectrometers are typically optimized for spectro-

scopy and routinely achieve sub-eV resolution below 1 keV [20], at the expense of low efficiency (figure 6). However, the efficiency can be improved by using a point-to-parallel X-ray optic before the diffraction grating with cone angles up to 24° [21]. The P/B ratio is typically set by elastically scattered incident beam.

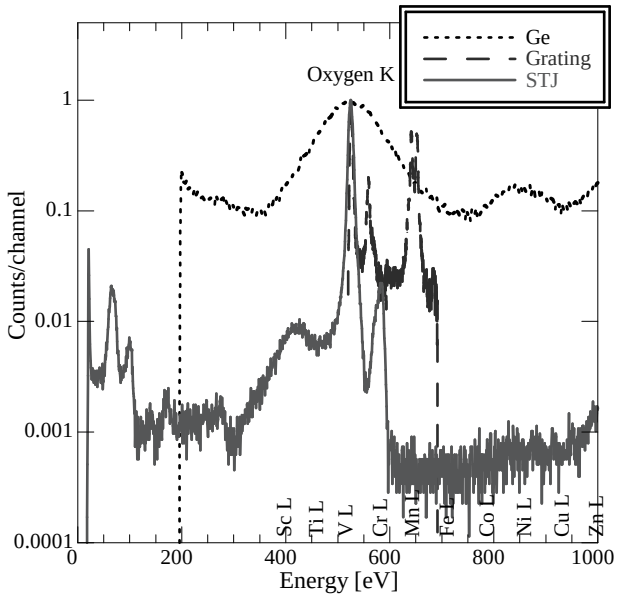

Fig.6.: Comparison of normalized detector response functions. The spectra are from a Ni-containing protein (Ge detector), a monochromatic 525 eV beam (STJ), and a MnO model compound (Grating). Labels on the x-axis correspond to the approximate L-series fluorescence energies for the first row transition metals [21]. Note the vicinity of the V and Cr lines with the oxygen K fluorescence at 525 eV.

D. Transition Metal L-edge Spectroscopy

We now apply the sensitivity analysis based on (1) to X-ray spectroscopy of dilute transition metals using signal rates according to (2) and the spectrometer characteristics of table 1. We assume an incident flux $I_0 = 10^{12}$ photons/s and an acquisition time $\tau = 15$ s per excitation energy for an XAS scan time of ~1 hour. Considering the increased μ_x at the absorption edges, we set $\mu_x(E_0)/(\mu_{tot}(E_0)+\mu_x(E_x))$ to 10^{-3} for a metal concentration of 1000 ppm, and use published values for the fluorescence yield ε_x, which varies between $8.4\cdot10^{-4}$ for Sc and $1.2\cdot10^{-2}$ for Zn L-edges [22]. The count rate is either constrained by the spectrometer characteristics or by the maximum signal rate from the sample. We also assume that the sample contains significant amounts of oxygen, that the only potential line overlap arises from the O K fluorescence at 525 eV, and that this line is 100 times stronger than the fluorescence from the transition element of interest.

Figure 7 shows the signal-to-noise ratio for the analysis of first-row transition metals with a metal concentration of ~1000 ppm for different spectrometer types. In general, the S/N ratio increases slightly for the heavier elements because of the higher fluorescence yield ε_x and thus higher signal rates, with lower S/N ratios for V, Cr and Mn whose emission lines are near the interfering oxygen K fluorescence at 525 eV. For the elements Sc and Fe to Zn, 30-element Ge spectrometers (diamonds) offer higher sensitivity than typical 9-pixel STJ-spectrometers, because they efficiently capture the weak signal with high S/N ratio as long as there are no large interfering fluorescence lines nearby. STJ spectrometers (circles) are favorable for the elements Ti to Mn because they can separate their weak metal fluorescence from the interfering O K line, with lower efficiency than Ge spectrometers, but sufficient to acquire XAS spectra with high S/N ratio within a ~1 hour scan. The 36-pixel detector upgrade significantly enhances the sensitivity of STJ spectrometers because of the higher detection efficiency and count rate capabilities (solid circles).

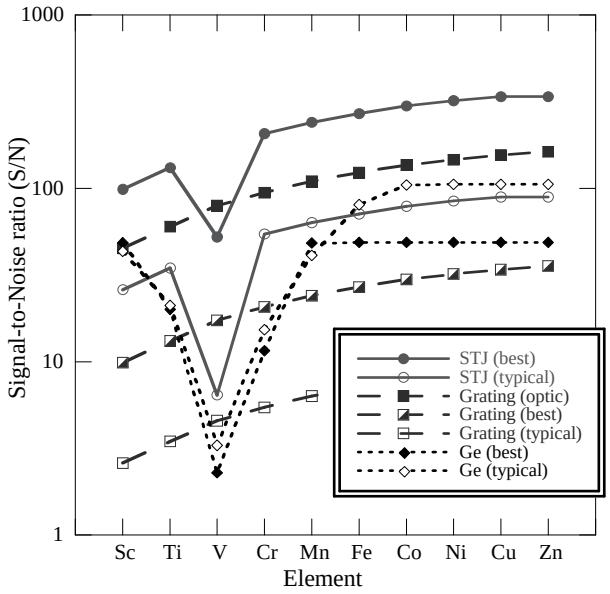

Fig 7. Signal-to noise ratio for analyzing L-series X-rays of first-row transition metals with a concentration of ~1000 ppm in data acquisition time of 15 s. Spectrometer parameters are taken from table 1.

Note that even the best single channel Ge spectrometer with an energy resolution of 60 eV and an area of 10 mm^2 does not provide higher sensitivity because of its limited count rate capabilities (which cause the S/N ratio to remain constant for the elements Mn to Zn in this simulation) and the spectral background from the electrode's dead layer.

Except for the case of severe line overlap between the V L and O K emission, grating spectrometers (squares) tend to be less favorable for the analysis of dilute specimens despite their high energy resolution because of their low detection efficiency. High efficiency X-ray focusing optics can partially alleviate this problem, although they could of course also be used to further improve the efficiency of STJ spectrometers.

IV. SUMAMRY AND OUTLOOK

Superconducting tunnel junction (STJ) X-ray spectrometers are being developed for the chemical analysis of dilute (~10 to ~1000 ppm) specimens by fluorescence-detected X-ray absorption spectroscopy (XAS). We have quantified the signal-to-noise ratio that different spectrometers can attain as a function of energy resolution, count rate capabilities and detection efficiency for samples with different metal concentrations and degrees of line overlap. As an example, we

have applied this quantification to the L-edge XAS of first-row transition metals. STJ spectrometers tend to be preferred over conventional high-purity Ge spectrometers for the analysis of the lighter elements Ti to Mn when oxygen fluorescence can cause a significant spectral background. STJs can also be used to analyze heavier elements, although current multi-element Ge spectrometers are more sensitive in that case because of their larger effective area. Future developments of STJ spectrometers will focus on further increasing their detection efficiency and sensitivity by improving the spectral purity of their response function and by developing large arrays. This will further increase the advantage that's STJ offer for fluorescence-detected soft X-ray absorption spectroscopy of dilute samples.

REFERENCES

[1] J. B. LeGrand et al., *Appl. Phys. Lett*., vol. 73, pp. 1295-1297 (1998).
[2] G. Angloher et al., *J. Appl. Phys.*, vol. 89, pp. 1425-1427 (2001).
[3] L. Li et al., *J. Appl. Phys.*, vol. 90, pp. 3645-3646 (2001).
[4] P. Verhoeve et al., *Opt. Eng*., vol. 41, pp. 1170-1184 (2003).
[5] S. Friedrich et al., *Rev. Sci. Inst*., vol. 73, pp. 1629-1631 (2002).
[6] J. Jaclevic et al, *Solid State Comm*., vol. 23, pp 679-682 (1977).
[7] T. Funk et al., *J. Am. Chem Soc*., vol. 126, pp. 88-95 (2004).
[8] V. Lordi et al., *Phys. Rev. Lett*., vol. 90, pp. 145505-145508 (2003).
[9] P. L. Ryder, *Scanning El. Microscopy*, vol. 1, pp. 273-280 (1977).
[10] P. J. Statham, in "*X-ray Spectrometry in Electron Beam Instruments*", pp. 101-125, Plenum Press, New York (1995).
[11] F. M. F. deGroot et al., *Phys. Rev. B*, vol. 42, pp. 5459-5468 (1990).
[12] S. P. Cramer et al., *J. Am. Chem. Soc*, vol. 113, pp. 7937-7940 (1991).
[13] Canberra Industries Inc., www.canberra.com.
[14] Gresham Scientific Instruments, www.gsinst.com.
[15] M. C. Lépy et al., *Nucl. Inst. Meth*, vol A439, pp. 239-246 (2000).
[16] J. B. le Grand et al., *Appl. Phys. Lett*., vol. 73, 1295-1297 (1998).
[17] S. Friedrich et al., *J. El. Spec. Rel. Phen*., vol. 101, pp. 891-896 (1999).
[18] S. Bechstein et al., *Spectrochim. Acta*, vol. B95, pp. 215-221 (2004).
[19] C. A. Mears et al., *Appl. Phys. Lett*., vol. 63, pp. 2961-2963 (1993).
[20] J. Nordgren, J. Juo, *J. El. Spec. Rel. Phen.*, vol. 101, pp. 1-13 (1999).
[21] Parallax Research Inc., www.parallax-x-ray.com.
[22] M. O. Krause, *J. Phys. Chem. Ref. Data*, vol. 8, pp. 307-327 (1979).